Chemical Engineering Science 310 (2025) 121544

Contents lists available at ScienceDirect

Chemical Engineering Science

journal homepage: www.elsevier.com/locate/ces

# Control of PLA chemical structures by using GMA and DCP during reactive processing and its influence on PLA foamability

Ana Beatriz Valim Suquisaqui [a,b], Lívia Maria Garcia Gonçalves [a,b], Laís Taguchi Possari [a,b], Eliada Andrade Silva [c], Benedito dos Santos Lima Neto [c], Rosario Elida Suman Bretas [b], Paulo de Tarso Vieira e Rosa [d], Sílvia Helena Prado Bettini [a,b,*]

[a] Federal University of São Carlos, Graduate Program in Materials Science and Engineering, Rodovia Washington Luiz, Km 235, SP-310, 13565-905 São Carlos, São Paulo, Brazil
[b] Federal University of São Carlos, Department of Materials Engineering, Rodovia Washington Luiz, Km 235, SP-310, 13565-905 São Carlos, São Paulo, Brazil
[c] São Paulo University, Chemistry Institute of São Carlos, Avenida Trabalhador São Carlense, 400, 13566-590 São Carlos, São Paulo, Brazil
[d] University of Campinas, Institute of Chemistry, Cidade Universitária Zeferino Vaz, 13084-862, Campinas, São Paulo, Brazil

ARTICLE INFO

*Keywords:*
PLA foam
Reactive processing
Supercritical fluids
Glycidyl methacrylate
Dicumyl peroxide

ABSTRACT

This study aimed to chemically modify poly(lactic acid), PLA, by reactive processing as a strategy to increase its melt strength, making it viable for producing foams. For this purpose, modification reactions were carried out in a Haake torque rheometer according to a $2^2$ factorial design, where the concentrations of dicumyl peroxide (DCP) and glycidyl methacrylate (GMA) were varied. The levels evaluated were 0.5 and 1.5 phr (peroxide concentration) and 1 phr and 3 phr (GMA concentration). Reference samples with a single reagent were also investigated. The modified PLAs were characterized, and foams were produced by incorporating supercritical $CO_2$ followed by fast depressurization. The results showed that the predominant reactions differed depending on the relative levels of peroxide and GMA, resulting in crosslinking, and/or insertion of branches, and/or linear reactions. Rheological analyses showed that PLA with low levels of peroxide and GMA (PLA_0.5_1) and high levels of both (PLA_1.5_3) displayed a more elastic behavior, which can be correlated to long chain branching formation with longer relaxation times. Consequently, these samples presented smaller cell sizes with homogeneous distribution, while unmodified and less branched PLA foams comprised coalescent and heterogeneous cells with thick walls. The study showed an optimization of the use of reagents once the sample containing the lowest levels of DCP and GMA presented the smallest cell size, attributed to the rheological properties and influence of crystallinity. As far as we know, the correlation between GMA and DCP concentrations on the final cellular structures of PLA foams has never been explored before.

## 1. Introduction

Polymeric foams are of particular interest due to their low density, which results in reduced material usage, along with other significant characteristics such as high protective effect in packaging, and thermal and sound insulation, among others (Ansari and Sheikh, 2023; Dong et al., 2023; Jin et al., 2019). Consequently, polymeric foams are used in various applications such as cushioning, packaging, insulation, purification, construction, household, scaffolds, etc. (Souza et al., 2023). In addition, recent literature has mainly investigated the behavior of the foaming process using supercritical carbon dioxide (sc-$CO_2$) as the physical blowing agent, which presents non-toxicity, non-flammability, low cost, and is chemically inert (Champeau et al., 2015; Gonçalves et al., 2024; Rojas et al., 2020). However, because of economic and logistic issues, polymeric foams generally present low recyclability, leading to irregular disposal and environmental pollution, mainly for single-use applications. Due to environmental concerns over the excessive use of fossil-based polymers, poly(lactic acid) (PLA) has gained prominence because it is a material obtained from renewable sources, biodegradable in compost conditions, biocompatible, and produced on a large scale (Hopmann et al., 2015). For this reason, it has been explored as an alternative to producing polymeric foams that mostly use polymers from fossil sources (Gonçalves et al., 2024).

One of the main disadvantages of PLA, however, is its low melt

* Corresponding author.
*E-mail address:* silvia.bettini@ufscar.br (S.H.P. Bettini).

https://doi.org/10.1016/j.ces.2025.121544
Received 6 January 2025; Received in revised form 12 March 2025; Accepted 16 March 2025
Available online 17 March 2025

strength, related to its linear chain structure, which, as a consequence, results in low elasticity and viscosity, avoiding the strain hardening, an essential property during the foaming process of semi-crystalline polymers (Lee, 2017). Nevertheless, the literature reports that, with appropriate modifications, it is possible to improve some characteristics of PLA to allow its foaming.

Dirlam et al. (Dirlam et al., 2019) used mono-, tri-, and tetrafunctional initiators in the polymerization of PLA in order to synthesize 3- and 4-arm star PLA. Compared to net PLA, 3- and 4-arm star PLA resulted in homogeneous and coherent foams, presenting lower density than linear PLA. Li et al. (P. Li et al., 2020b) also modified PLA in the presence of peroxide and different monomers such as 4-butylene diacrylate (BDDA), trimethylolpropane tri-acrylate (TMPTA), and pentaerythritol tetra acrylate (PET4A). They identified an increase in molar masses for all formulations, even when compared to the modification using only peroxide. The authors affirm that the presence of monomers improves the insertion of long-chain branches, which results in higher molar masses and improves rheological properties, leading to PLA foams with thin cell walls and a high expansion ratio. In contrast, the neat PLA foam modified only with peroxide had thick cell walls and a low expansion ratio.

Standau et al. (Standau et al., 2019b) conducted a literature review and observed different types of chain extenders most commonly used for the chemical modification of PLA based on their reactive functional groups. The authors highlighted monomers containing epoxy, isocyanate, anhydride, oxazoline, carbodiimide, and phosphate groups. Among these monomers, those with the epoxy group were the most used for chemical modification of PLA to improve characteristics and enable the foaming process (Auras et al., 2010; Corre et al., 2011; Standau et al., 2019b).

One of those was glycidyl methacrylate (GMA), a bifunctional monomer with epoxy and acrylic groups. The epoxy group of GMA can react with other groups, such as hydroxyls and carbonyls, while the acrylic group can graft GMA into the polymeric chain via free radicals (Xu et al., 2012). Those radicals can be obtained by using peroxides as initiators, where at processing temperatures, the ROOR bond splits, generating peroxyl radicals (RO●), which abstract a hydrogen atom from the polymeric chain, creating a macroradical (Hamielec et al., 1991). In this way, the stability or relative reactivity of the radicals is related to the peroxide structure, and its decomposition rate can be measured through its half-life time ($t_{1/2}$).

Some works have highlighted the chemical modification of PLA as an alternative to chain extension. Rigolin et al. (Rigolin et al., 2021) modified PLA using GMA in the presence of peroxide and observed an increase in molar masses depending on the concentration of both chemicals. The authors observed that increasing the concentration of GMA did not enhance the molar mass at the same proportion, probably because the high concentration of monomer enabled the formation of a second phase (monomer) into the PLA phase. However, this investigation did not perform modified PLA foaming, as well as other studies that used GMA and DCP in PLA chemical modification (Kangwanwatthanasiri et al., 2015; Thanh et al., 2016).

For the PLA foaming purpose, studies are concentrated on using GMA as a chain extender in the form of random copolymers such as polystyrene/poly(glycidyl methacrylate) (by sc-$CO_2$) (Zhou et al., 2015), ethylene/glycidyl methacrylate (sc-$CO_2$) (Cui et al., 2022; Y. Li et al., 2020), ethylene/acrylic ester/glycidyl methacrylate (azodicarbonamide) (M. Li et al., 2021), styrene/cryolinitrile/GMA (by sc-$CO_2$) (Y. Li et al., 2019). Another strategy is grafting GMA in other polymers to process with PLA and produce foams, e.g., poly(ethylene octane) grafted with GMA by sc-$CO_2$ (Wang et al., 2018; X. Wang et al., 2019) or azodicarbonamide (Forghani et al., 2016). These strategies are also improving rheological properties to produce foams. For example, Li et al. (Y. Li et al., 2020) modified PLA using an ethylene glycidyl methacrylate random copolymer at several concentrations without an initiator; by Soxhlet extraction, the presence of crosslinking in the modified samples was observed, which they concluded was essential to the improvement of elasticity in the melt state and thus, to the ability to expand the material. According to the authors, the higher the concentration of chain extender, the higher the percentage of crosslinking and the complex viscosity. This led to cell growth limitation because the increase in viscosity also increases the resistance to material expansion.

However, rheological properties are not the only factors that influence polymer foamability. Crystallization during the foaming process is crucial as it directly impacts the dissolution of $CO_2$ within the PLA matrix. $CO_2$ primarily dissolves in the amorphous phase, where the crystalline regions act as barriers to molecular diffusion. Furthermore, crystallization can influence cell nucleation, with crystals acting as nucleation sites, thereby controlling the foam's cellular structure (Yan et al., 2020).

During the gas saturation process with sc-$CO_2$, the gas molecules lubricate the system, making the polymer chains more mobile. This explains that even at temperatures below the crystallization temperature of PLA, the material crystallizes in the presence of sc-$CO_2$ (Kuska et al., 2019). This is important for the foaming process because the crystallization of the material during the $CO_2$ saturation phase will determine whether the expansion will occur in the presence or absence of crystals, thus characterizing the type of cell nucleation as homogeneous or heterogeneous.

For example, Yang and colleagues (Yang et al., 2019) carried out differential scanning calorimetry (DSC) analyses on the foams to understand whether crystallization occurred during the foaming process with sc-$CO_2$. They observed that at a high foaming temperature (120 °C), the foams presented no melting peak, which showed no crystallization during gas saturation. For temperatures between 70 and 110 °C, DSC analysis resulted in a melting peak with no crystallization peak, which was associated with the complete crystallization of the material during the foaming process.

In this sense, studying and understanding the factors that influence the cellular structures of polymeric foams is crucial because they will affect the final properties of the foam. Small, closed cells with uniform distribution generally exhibit superior mechanical properties (Banerjee and Ray, 2020). Thermal insulation can also be increased by increasing the expansion ratio since the thermal conductivity of the air is much lower than that of the matrix (Wang et al., 2017; L. Wang et al., 2019). Foams with open cells, for example, have lower mechanical properties than closed cells but present a high absorption and acoustic insulation capacity (Banerjee and Ray, 2020; Shau-Tarng Lee; Chul B. Park; N.S. Ramesh, 2007).

This work aimed to chemically modify PLA using GMA and dicumyl peroxide as an initiator. A $2^2$ experimental design was used to evaluate the influence of the ratio peroxide/GMA on the PLA chain extension (by linear growth, branching, or crosslinking) and to observe their impact on the PLA foams cellular structure, prepared using supercritical $CO_2$ as a blowing agent. This investigation provides an optimization on the use of reagents in the chemical modification of PLA aiming at the production of bio-based foams and, as far as we know, the correlation between GMA and DCP concentrations on the final cellular structures of PLA foams has never been explored before.

## 2. Materials and Methods

### 2.1. Materials

PLA Ingeo Biopolymer 4043D was purchased from NatureWorks LLC (MRF 6 g/10 min, 210 °C, 2.16 kg), with a melting temperature $T_m$ between 145 °C and 160 °C. The manufacturer did not inform the % of D content, but it was assured that it was free of additives and hydrolysis stabilizers (which could influence the chain extension reactions). The GMA and dicumyl peroxide (DCP, half-life time 30 s at 180 °C) were purchase from Sigma-Aldrich (both structures are presented in Fig. 1); both materials were used as received.

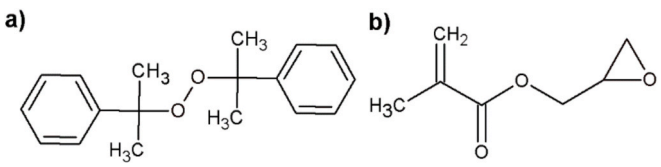


**Fig. 1.** Chemical structure: (a) DCP; (b) GMA.

### 2.2. Chemical modification of PLA

Chemical modification of PLA was conducted by reactive processing in a Haake torque rheometer, model Rheomix 600, equipped with roller rotors, following a $2^2$ factorial design; the GMA and DCP concentrations, ($C_{GMA}$) and ($C_{DCP}$), respectively, were varied at 2 levels and measured in parts per hundred resin (phr), as shown in Table 1. This experimental design was based on work by Rigolin and collaborators (Rigolin et al., 2021), whose results showed that the modification using 1 phr of DCP and 2 phr of GMA was more efficient in increasing the molar mass of neat PLA. Thus, this formulation was used as a reference, shifting the peroxide levels by 0.5 phr and reducing the GMA concentration since high concentrations generated a second phase and reduced the interface for reactions. Process conditions were as follows: temperature of 180 °C, rotation of 50 rpm, reaction time of 6.5 min, under a nitrogen atmosphere. The addition of DCP and GMA was carried out between 80 and 90 s. PLA was dried in a vacuum oven at 70 °C for 4 h before processing. Table 1 presents the nomenclature of the samples.

### 2.3. Characterization

#### 2.3.1. Size exclusion Chromatography (SEC)

The molar mass was obtained in a Viscotek_HT-GPC size exclusion chromatograph with a refractive index detector. The samples were solubilized in tetrahydrofuran (THF) at 45 °C; the injection volume was 200 µL, at a concentration of 5 mg/mL. All samples were previously purified to remove residual monomers and/or unreacted oligomers by previously drying them for 4 h in a vacuum oven at 70 °C, dissolving in HPLC grade chloroform at room temperature for 24 h, and then precipitating in HPLC grade ethyl alcohol.

#### 2.3.2. Determination of acids groups

Purified samples were dried in a vacuum oven (4 h at 70 °C); the percentage of acid groups was determined by titration. PLA (0.5 g) was dissolved in chloroform (50 mL) at room temperature and titrated using ethanolic KOH solution with a concentration of 0.04 M. The reverse titration was done in isopropanol HCL solution at a concentration of 0.04 M. Phenolphthalein was used as the indicator. The percentage of acid groups (% acidity) was calculated from:

$$\%acidity = \left(\frac{\mathbf{V_e}^{*}\mathbf{C_{KOH}}^{*}\boldsymbol{M_{g.a}}}{\mathbf{m_a}}\right) \quad (1)$$

where $V_e$ is the equivalent volume of KOH added ($V_{KOH} + V_{excess}$-$V_{HCl}$), $C_{KOH}$ is the molar mass concentration of KOH, $M_{ga}$ is the molar mass of the PLA acid group (45 g/mol), and $m_a$ is the mass of the sample.

#### 2.3.3. Rheological analysis

Rheological data was obtained using a tension-controlled TA Instruments AR-G2 rheometer with parallel plates geometry (d = 25 mm, gap between plates = 1 mm). The steady-state analysis (between shear rates of 0.01 and 100 $s^{-1}$) and the small amplitude oscillatory shear properties (between angular frequency of 0.05 and 500 rad/s), were measured at 180 °C and under a nitrogen atmosphere. Unpurified samples were used for this characterization, being vacuum-dried before the experiment (4 h at 70 °C).

**Table 1**
Nomenclature of samples with different DCP and GMA concentrations.

| Identification | $C_{DCP}$ (phr) | $C_{GMA}$ (phr) |
|---|---|---|
| PLA_0.5_1 | 0.5 | 1 |
| PLA_0.5_3 | 0.5 | 3 |
| PLA_1.5_1 | 1.5 | 1 |
| PLA_1.5_3 | 1.5 | 3 |

#### 2.3.4. Differential scanning calorimetry (DSC)

DSC was performed in a TA Q2000 DSC. A first heating cycle at a heating rate of 10 °C/min, between 0 °C and 200 °C, under nitrogen gas flow was applied to dried samples (4 h at 70 °C); after attaining 200 °C, the samples were kept at that temperature for 1 min and then were cooled down to 25 °C. A second heating cycle was applied at 10 °C/min, between 0 °C and 200 °C.

#### 2.3.5. Crosslinking content

The crosslinking content of the unpurified samples was determined by extracting the soluble fraction with boiling chloroform and using a Soxhlet extractor for 6 h. All samples and filters were vacuum-dried (4 h at 70 °C) and weighed before extraction. Finally, all samples were left for solvent evaporation and vacuum-dried at 70 °C for 5 h. The calculation of the crosslinking percentage was obtained as follows:

$$\%Crosslinking = \frac{m_f - m_{filter}}{m_{PLA\_i}} \quad (2)$$

where $m_f$ is the mass of the remaining PLA and the filter (both dried) after extraction, $m_{filter}$ is the mass of the dried filter before the extraction, and $m_{PLA\_i}$ is the mass of dried PLA before the extraction.

#### 2.3.6. Nuclear Magnetic Resonance (NMR) analysis

$^{1}H$, $^{13}C$, and HSQC (500 MHz) NMR analysis were performed on a NMR Spectrometer, from Agilent Technologies, model 500/54 premium shielded. To identify the functional groups involved in the branching reaction and for mechanistic studies. Spectra were obtained at 26 °C in $CDCl_3$.

### 2.4. Foaming of modified PLA

The foaming process was done in an in-house device, using supercritical $CO_2$ as the blowing agent. The device consisted of a high-pressure pump of $CO_2$, an oven, and a hermetical cylinder, as shown in Fig. 2.

The process can be divided into 3 steps: i) sc-$CO_2$ saturation, ii) lowering of temperature, and iii) fast depressurization. The modified PLA samples (approximately 0.4 g) were inserted in a cylindrical Teflon

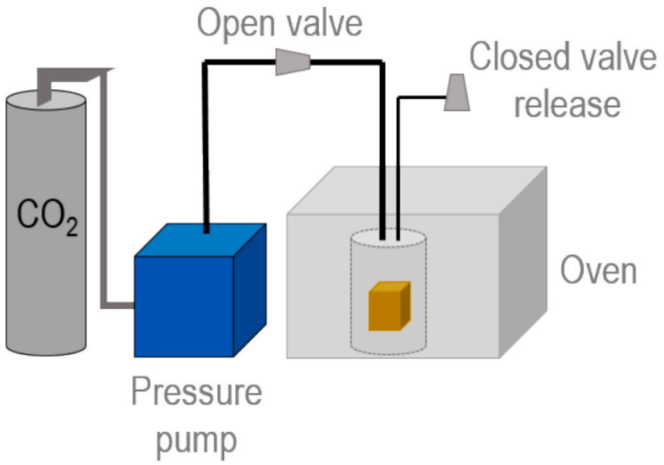


**Fig. 2.** Scheme of the in-house foaming device.

mold that evolved by a hermetic cylindrical system; the sample was then left to be saturated for 1 h at 150 °C and 20 MPa. The second step was lowering the temperature to 90 °C for 30 min and 20 MPa. This decrease in temperature is necessary to increase the material viscosity, once in the first step, the high temperature (close to $T_m$) hinders the expansion due to low viscosity. Finally, the pressure was released quickly by opening the valve. The foamed samples were removed from the cylinder and left to cool at room temperature.

### 2.5. Characterization of PLA foams

#### 2.5.1. Scanning electron Microscopy (SEM)

A scanning electron microscope, a MEV FEI Magellan 400L microscope, was used to analyze foam structures and compare cell morphology. The foams were cryo-fractured using liquid nitrogen and, afterward, gold-sputtered.

#### 2.5.2. Foams characterization

The densities of the foamed and non-foamed samples were determined using the water displacement method (ASTM D792-20), in triplicate, with each one measured five times. The volumetric expansion ratio (VER) was calculated by the ratio between the density of the non-foamed material and the density of the foamed material. The cell structures (cell size and cell density) were characterized using the ImageJ software. Cell density (N) was calculated using Eq. (3), with at least 100 cells measured for each sample.

$$N = \left(\frac{n}{A}\right)^{3/2} \times VER \tag{3}$$

where N is the cell density, n is the number of cells in a known area A and ϕ is the expansion ratio.

### 2.6. Statistical analysis

When appropriate, statistical tests ANOVA, followed by Tukey's multiple comparisons test, were carried out with a 95 % confidence level ($p < 0.05$ = significance level).

## 3. Results and discussion

### 3.1. Torque results during chemical modification of PLA

As torque rheology was used for reactive processing, the process was evaluated as a function of the reaction time (which was set to be higher than five times the half-life of the peroxide – 30 s at 180 °C (Rigolin et al., 2019)). The torque *versus* time curves of the formulations produced from the experimental design are shown in Fig. 3.

For all the curves shown, it is possible to observe a discontinuity near 1.5 min, when the reagents were added to the mixture. The addition of GMA to PLA (Fig. 3a), in the absence of peroxide, did not modify the torque of the PLA. This can be explained by the fact that the GMA cannot be grafted onto the PLA chain in the absence of peroxide. However, a reaction between the epoxy group of the GMA and the carboxyl or hydroxyl groups of the PLA chain ends can occur, as illustrated in Fig. 4. On the other hand, the GMA that did not react during processing can remain present in the polymer mass, behaving like a lubricant, which can explain the slight decrease in the torque of the material and, consequently, the lower viscosity of the formulation with 3 phr of GMA.

Regarding the addition of peroxide to PLA, in the absence of GMA, it is observed that unlike the addition of GMA, the presence of peroxide resulted in a significant increase in torque compared to pure PLA (Fig. 3a), even at the lowest level of the experimental design (0.5 phr). This suggests that an extension of the PLA chain occurred by branching and/or crosslinking, promoted by this initiator, which led to an increase in the viscosity of the medium and, consequently, an increase in the torque. Fig. 3b shows the graphs for PLA modified with both reagents simultaneously, peroxide and GMA, at lower and upper levels.

It is observed in Fig. 3b that, within the experimental error, the lower-level formulations of DCP (PLA_0.5_1 and PLA_0.5_3) had similar torque to those of the neat PLA sample (PLA_0_0). However, the 1.5 phr peroxide and 1 phr GMA formulation (PLA_1.5_1) displayed an increasing torque during processing with a maximum of 30 N.m. Removing that material from the torque rheometer was difficult due to its solidification, which may indicate chain extension with a predominance of crosslinking. When the concentrations of peroxide and GMA concentration were maximum (PLA_1.5_3), an increase in torque during the processing was also observed, but at a lower level than the PLA_1.5_1 formulation. It can be highlighted that large structural variations can also display similar torques. Therefore, SEC analysis, acid group

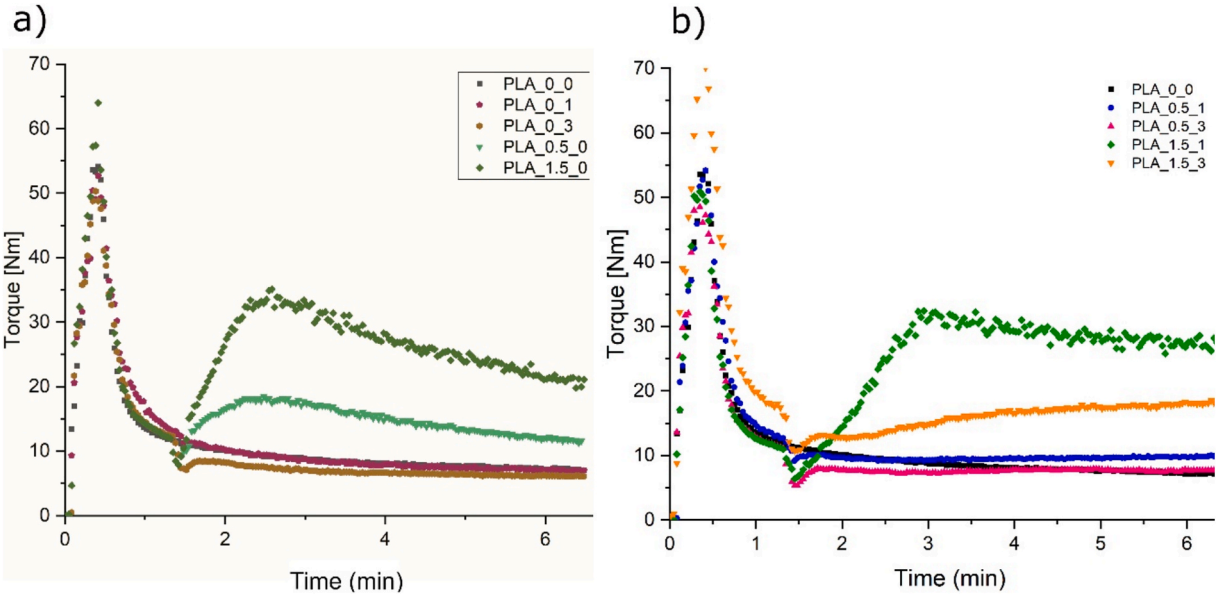


**Fig. 3.** Reactive processing of the formulations: (a) reference formulations (b) experimental design $2^2$. Code: PLA_$C_{DCP}$_$C_{GMA}$.

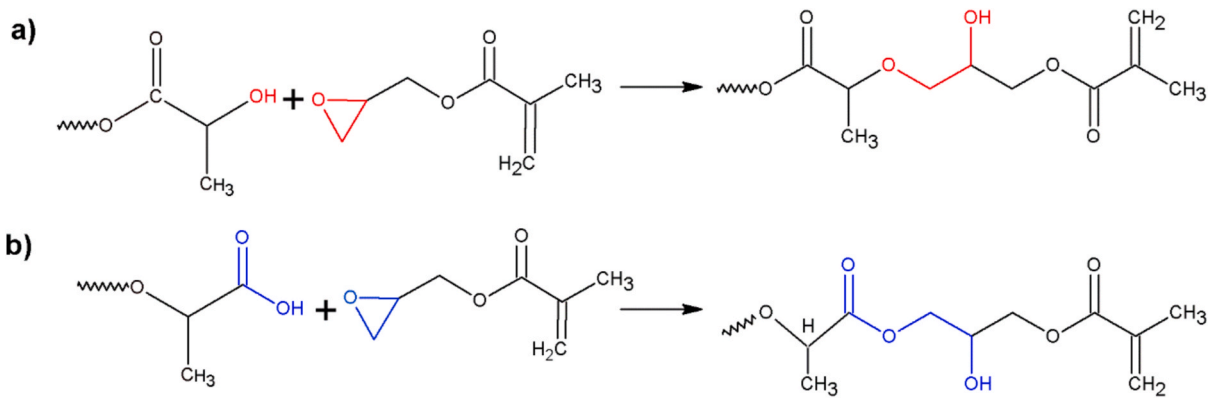


**Fig. 4.** Possible reactions between the epoxy group present in PLA-g-GMA and the a) hydroxyl group at the end of the chain of another PLA molecule and b) carboxylic acid group at the end of the chain of another PLA molecule.

titration, and Soxhlet extraction were carried out to investigate possible changes in the modified structures.

### 3.2. Influence of chemical modification on final chemical structures

Degradation can also occur during reactive processing. As can be observed in Table 2, processed PLA presents a lower molar mass than PLA pellets. This degradation results from high temperatures, shear stresses, oxygen presence, and hydrolysis (small water concentrations in PLA can be present even after drying). All these factors can lead to a decrease in molar mass during processing. In addition, it is possible to observe that the acidity of processed PLA is much higher than that of the PLA pellets since the hydrolysis of ester bonds during processing can produce more acid groups.

To understand the possible reactions occurring during the reactive processing, Fig. 5 shows reaction mechanisms that may happen during the chemical modification.

When the reactions are carried out in the presence of peroxide, its dissociation forms two peroxyl radicals (Fig. 5, R1), which abstract hydrogens from the secondary carbon of the PLA chain (Rigolin et al., 2021), resulting in PLA macroradicals (Fig. 5, R2). Two routes can stabilize these macroradicals: i) PLA chain scission (Fig. 5, R3), which decreases molar masses; ii) recombination between PLA macroradicals (Fig. 5, R4), which can lead to a decrease in the free volume of chains and depending on the intensity of recombination, it can lead to a crosslinked structure. When PLA, peroxide, and GMA are present, other reactions can also occur: iii) grafting of GMA molecules onto PLA (Fig. 5, R5′), resulting in short, branched structures. The epoxy groups present in GMA structure likely react to both hydroxyls and carboxylic end groups of PLA (Auras et al., 2010; Corre et al., 2011; Standau et al., 2019b). However, reactivity with carboxylic groups is higher than with hydroxyls. This last reaction can result in long chain branches (Fig. 3, R5′′).

All the mentioned reactions are competitive, and the intensity of each reaction will depend on the concentration of peroxide and GMA (Rigolin et al., 2021).

From Table 3, it is possible to note that the analysis of formulation PLA_1.5_0 (upper level of peroxide) and PLA_1.5_1 (upper level of peroxide and lower level of GMA) was not done since both were insoluble in chloroform or THF. For those samples, a gel behavior was observed when in solution, suggesting possible crosslinking reactions. The occurrence of crosslinking in PLA in the presence of peroxide has already been reported in the literature. Li et al. (P. Li et al., 2020a) explain that linear peroxides form crosslinked structures, while cyclic peroxides form mainly branched structures. Södergård et al. (Södergård and Stolt, 2002) also stated that the use of linear peroxides in concentrations between 0.1 % and 0.25 % promotes branched reactions; however, above 0.25 %, it is possible to observe crosslinking reactions. To confirm this statement, Soxhlet extraction was performed for 6 h; Fig. 6 presents the effect caused by the chemical modification using only peroxide in PLA.

As shown in Fig. 6, the higher the peroxide concentration, the higher the level of PLA crosslinking (for 0.5 phr and 1.5 phr, the crosslinking percentage was 56.2 % and 99.3 %, respectively). This result is mainly due to the increase in the concentration of PLA macroradicals formed as the concentration of peroxide increases. The higher the concentration of PLA macroradicals, the greater the degree of recombination between those macroradicals, which leads to the formation of a crosslinked network of PLA chains. Due to the high level of crosslinking, sample 1.5_0 was not analyzed. Sample 0.5_0, on the other hand, was analyzed by filtering out the crosslinked portion.

When GMA is added to the reaction medium, there is a competition between the recombination of PLA macroradicals and the grafting of GMA onto the PLA macroradical. The preferential reaction will result from the relative concentrations of peroxide and monomers in the

**Table 2**
Results of SEC, titration of acid groups, and Sohxlet extraction.

| Sample | Peroxide concen-tration (phr) | GMA concen-tration (phr) | $\overline{M}_n$(SEC_RI) (g/mol) | $\overline{M}_w$(SEC_RI) (g/mol) | PDI | % acidity |
|---|---|---|---|---|---|---|
| 4043D_pellet | 0 | 0 | 127,462 | 202,946 | 1.5 | $0.001 \pm 0.192^{b,c}$ |
| PLA_0_0 | 0 | 0 | 117,421 | 180,267 | 1.5 | $0.107 \pm 0.43^{a}$ |
| PLA_0_1 | 0 | 1 | 95,329 | 167,904 | 1.8 | $0.009 \pm 0.177^{b,c,d}$ |
| PLA_0_3 | 0 | 3 | 108,003 | 183,003 | 1.7 | $0.008 \pm 0.077^{d,e}$ |
| PLA_0.5_0 | 0.5 | 0 | 104,671* | 268,643* | 2.6 | $0.018 \pm 0.223^{*b}$ |
| PLA_1.5_0 | 1.5 | 0 | – | – | – | – |
| PLA_0.5_1 | 0.5 | 1 | 127,790 | 218,030 | 1.7 | $0.013 \pm 0.115^{b,c,d,e}$ |
| PLA_0.5_3 | 0.5 | 3 | 123,580 | 223,141 | 1.8 | $0.004 \pm 0.086^{c,d,e}$ |
| PLA_1.5_1 | 1.5 | 1 | – | – | – | – |
| PLA_1.5_3 | 1.5 | 3 | 188,280 | 487,090 | 2.6 | $0.001 \pm 0.066^{e}$ |

* Soluble phase of the formulation.

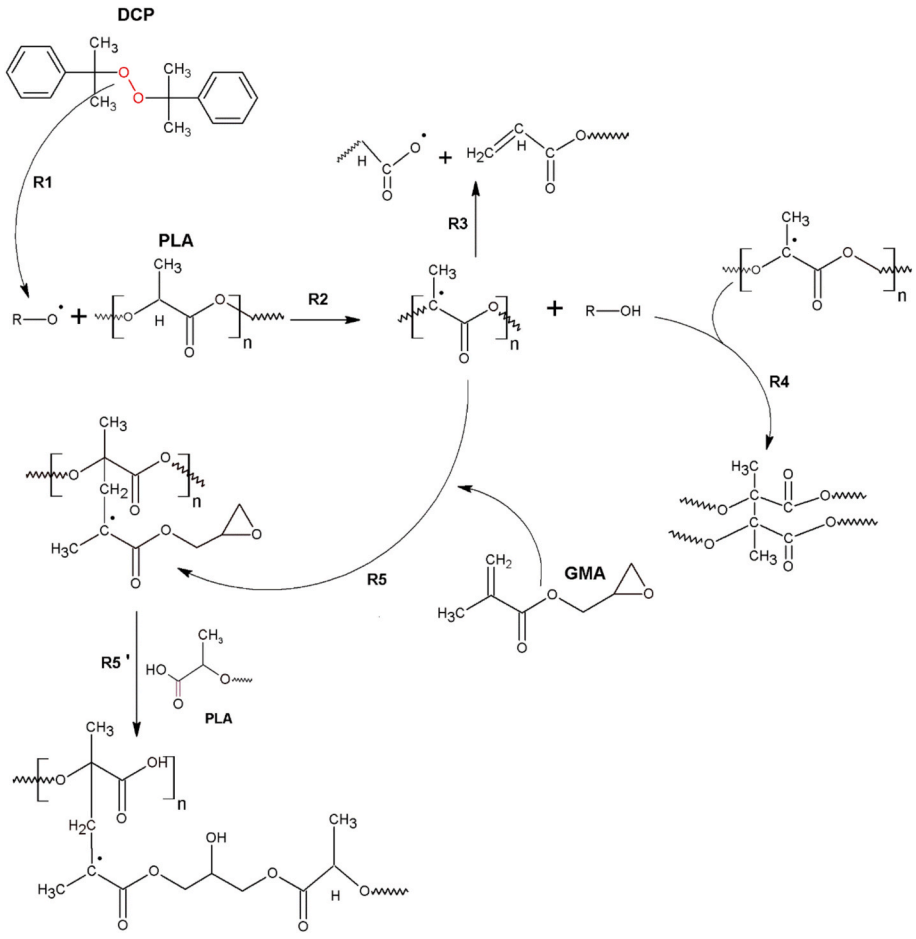


**Fig. 5.** Reaction mechanisms for PLA chemical modification, where: R1: Decomposition of DCP into two peroxyl radicals; R2- Formation of PLA macroradical in the presence of a peroxide; R3- Stabilization of PLA macroradical by chain scission; R4- Stabilization of PLA macroradical by recombination between different PLA macroradicals; R5 – Stabilization of PLA macroradical by insertion of GMA monomer; R5′ – Linear chain extension of branched GMA after reaction between epoxy group from GMA and carboxylic group from PLA.

**Table 3**
Crosslinking percentage of the samples.

| | | Crosslinking percentage | | |
|---|---|---|---|---|
| | | GMA (phr) | | |
| | | 0 (absense) | 1 (low level) | 3 (high level) |
| Peroxide (phr) | 0 (absense) | 0 %[c] | – | – |
| | 0.5 (low level) | 56 %[b] | 0.1 %[c] | 0.2 %[c] |
| | 1.5 (high level) | 99 %[a] | 100 %[a] | 0.3 %[c] |

reaction medium. Table 3 shows the occurrence of crosslinking for the samples.

For the lowest peroxide level (0.5 phr), adding GMA at both the upper and lower levels reduced the crosslinking percentage from 56 % to values close to 0 %. Furthermore, as observed in Table 2, both formulations had an increase in molar mass compared to pure PLA, indicating that chain extension occurred mainly through the insertion of branches (Fig. 5, R5) and the reaction between PLA and GMA chain ends (Fig. 4). In addition, it can be seen that the increase in GMA concentration from 1 phr to 3 phr increased $\overline{M}_w$ by approximately 8 % and $\overline{M}_n$ by 18 % suggesting that, for this amount of macroradicals, the higher monomer concentration increased the likelihood of grafting occurring on the PLA macroradicals, in addition to the reactions between the PLA and GMA chain ends. This result can be validated by the acidity content of the samples since GMA will react preferentially with the acid groups of PLA. Sample 0.5_3 had the greatest increase in molar mass and the lowest percentage of acidity among the samples with a low peroxide level,

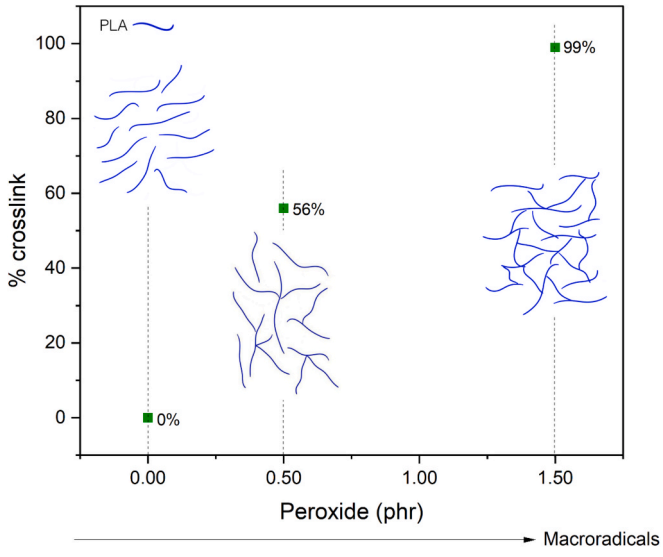


**Fig. 6.** Percentage of crosslinking structures obtained by Soxhlet extraction during 6 h at two concentrations of peroxide (0.5 and 1phr).

indicating the effectiveness of the reaction between PLA and GMA. Under these conditions, recombination reactions between macroradicals are less likely to occur. Contrarily, when the concentration of GMA in

the medium is low, the predominant reactions will be recombination between PLA macroradicals, concomitantly with GMA grafting reactions, in which the latter will occur to a lesser extent.

For the higher peroxide level (1.5 phr) the concentration of GMA was decisive for the balance between crosslinking and branching reactions. As can be seen in Table 3, the addition of 1 phr of GMA led to complete crosslinking of the sample (100 %), while the addition of 3 phr of GMA produced the same crosslinking content as the samples with the lower level of peroxide (0 %). This result suggests that the amount of PLA macroradicals formed was very high when the GMA concentration was at its lowest level (1 phr), which may have further favored crosslinking formation in the sample as a result of macroradicals recombination. On the other hand, the addition of GMA at a higher concentration (3 phr) was enough for the monomer to be grafted onto the PLA macroradicals, leading to the insertion of branches and, therefore, reducing the recombination between macroradicals that lead to the crosslinking of the material. For this formulation (1.5_3), the increase in $\overline{M}_w$ compared to pure processed PLA was approximately 170 %, and the acidity content was the lowest among the modified samples.

To synthesize the correlations between concentrations of DCP and GMA, Fig. 7 shows possible structures formed due to the reactive process.

NMR analyses were carried out to confirm the reaction assumptions, and the spectra are presented in the Supplementary Material (SI-1). As the analyses were carried out in solution and the abundance of $^{13}C$ is 1.1 % and that of $^{1}H$ is 99 %, changes can be observed in the chemical shifts of the secondary hydrogens of PLA and those of GMA. It can be inferred from comparing the PLA and modified PLA's spectra that in different proportions of peroxide and GMA, different products are formed. Analysis of sample PLA_0.5_1 indicates the grafting of GMA onto PLA macroradicals, followed by chain extension by reaction with carboxylic end groups. This product is present in all formulations. The differences between the formulations are due to the presence of other products. In the case of sample PLA_0.5_3, unreacted GMA is present in the formulation, confirming the excess of GMA, which may have lubricated the system. In the case of PLA_1.5_3, in addition to the grafted PLA, the PLA chain is terminated with two isomers. The entire discussion of chemical shifts and proposed mechanism is presented in the Supplementary Material.

Thermal analyses with DSC were performed to better understand the chemical modification, and the results are presented in Table 4. For all modified samples, $T_g$ was shifted to lower temperatures, as well as $T_m$. Furthermore, it was possible to observe that the crystallinity also decreased, mainly for formulation PLA_1.5_3, which presented a higher increase in molar mass, according to SEC results. Although small differences in $T_g$ and $T_m$, these results can confirm structural modifications, with the possible insertion of branches, which could increase free volume and, as a consequence, result in lower $T_g$ values, less structural organization, less perfect crystals, and lower crystallinity, compared to neat PLA.

Although the $\overline{M}_w$ and $\overline{M}_n$ values were very similar for the reactions conducted at the lower peroxide level (PLA_0.5_1 and PLA_0.5_3), the percentage of acid groups was higher for the PLA_0.5_1, and also the torque values. Therefore, rheological analyses were carried out in the steady state and oscillatory regimes to better understand these differences.

As can be seen from Fig. 8a, the PLA_1.5_3 formulation had a higher viscosity and a higher first normal stress difference (N1) than the other formulations at all shear rates; however, it attained a pseudoplastic behavior at lower shear rates. It is worthwhile to point out that long-chain branching (LCB) can increase both viscosity and elasticity (Bianchin et al., 2021) due to the formation of further entanglements. The earlier attainment of pseudoplastic behavior can be credited to its higher polydispersity. Therefore, long chain branches were probably formed by adding 1.5 phr of peroxide and 3 phr of GMA, as it shown in Fig. 7. However, when comparing the PLA_0.5_1 and PLA_0.5_3 formulations, which have very similar molar masses and polydispersity, it was observed that the viscosity at the Newtonian plateau ($\eta_0$) of the PLA_0.5_1 and the N1 were much higher than of the PLA_0.5_3 formulation. The difference between both formulations is the added amount of GMA.

The molar masses of those two formulations were very similar. The molar mass of the PLA_0.5_1 was only 3 % higher than the molar mass of the PLA_0.5_3 (within the experimental error); however, the $\eta_o$ of formulation PLA_0.5_1 (approx. 5 X $10^4$ Pa.s) was 416 % higher than the $\eta_o$ of formulation PLA_0.5_3 (approx. 1.2 X $10^4$ Pa.s). A very slight increase in molar mass would not produce such a high increase in viscosity (recalling that for linear polymers, $\eta_o \sim M^{3.4}$). Therefore, the increase in viscosity and elasticity of the PLA_0.5_1 was due to concurrent reactions between macroradical recombination and grafting of GMA onto PLA with subsequent reaction via epoxy group with PLA chain ends. When the concentration of GMA increased (PLA_0.5_3), the grafting reaction

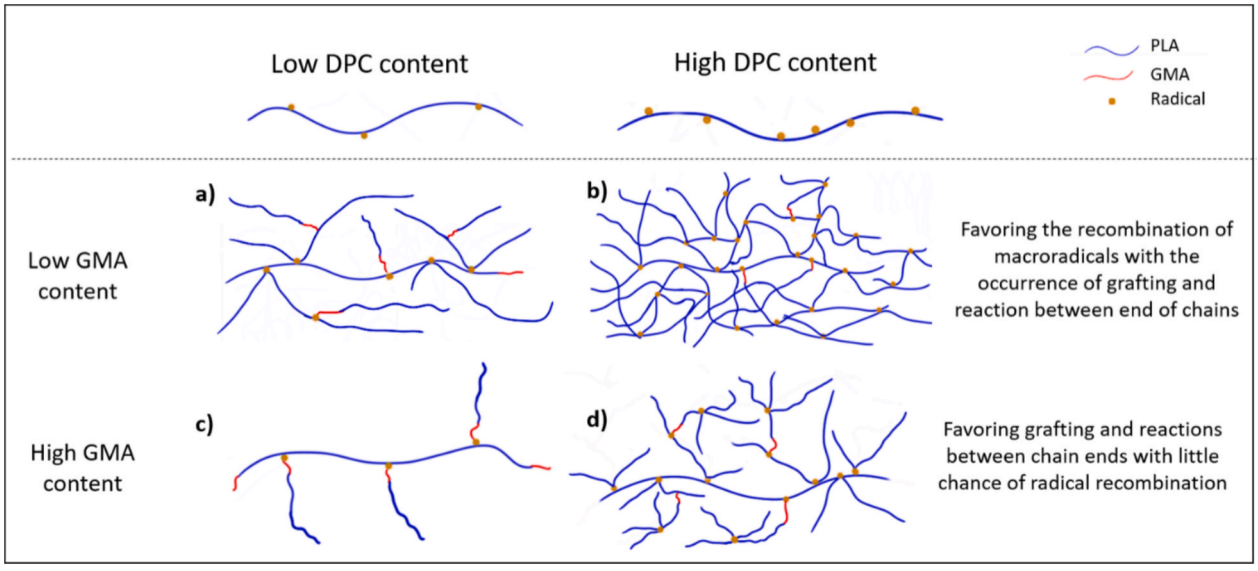


**Fig. 7.** Possible chain structures formed as a result of variation of DCP and GMA concentration during the reactive process, where: a) represents sample 0.5_1; b) sample 1.5_1 which presented crosslinked structure; c) sample 0.5_3 and; d) sample 1.5_3.

**Table 4**
Thermal results by DSC analysis.

| Samples | $T_g$ | $T_{cc}$ | $T_m$ | $\Delta H_{cc}$ (J/g) | $\Delta H_m$ (J/g) | % crystallinity | % maximum crystallinity potential |
|---|---|---|---|---|---|---|---|
| PLA_0_0 | 60.7 | 113.7 | 150.0 | 23.8 | 24.8 | 1.10 | 23.1 |
| PLA_0.5_1 | 59.3 | 116.9 | 147.4 | 18.3 | 18.9 | 0.95 | 18.9 |
| PLA_0.5_3 | 57.3 | 117.4 | 148.2 | 20.0 | 20.3 | 0.89 | 20.5 |
| PLA_1.5_3 | 57.5 | 121.8 | 145.5 | 9.5 | 9.3 | 0.81 | 9.4 |

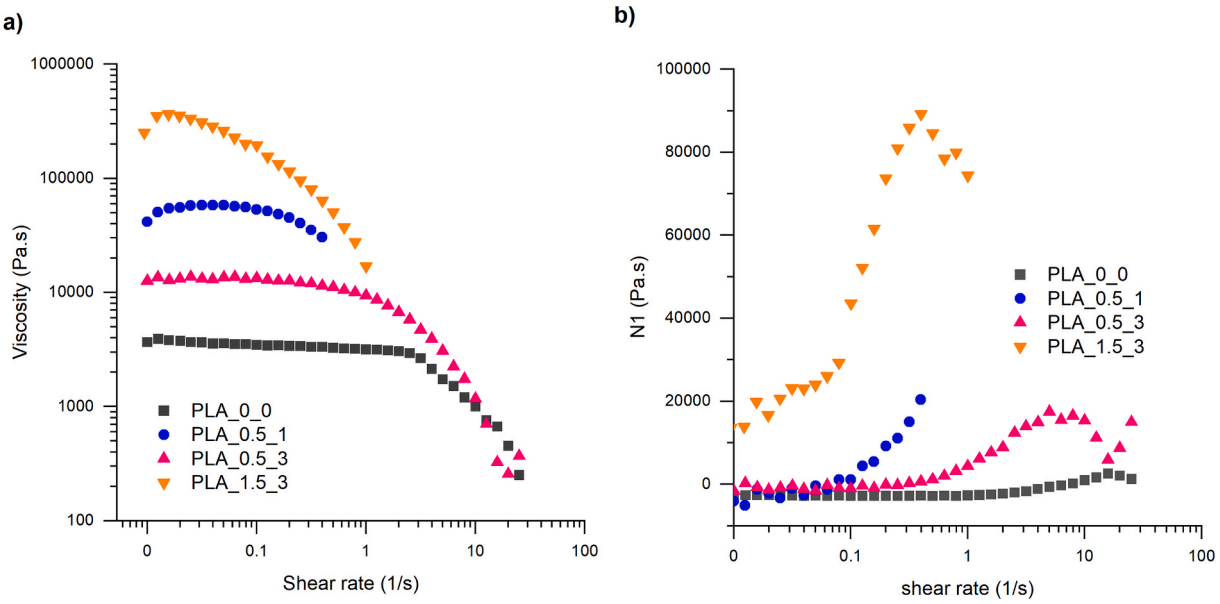


**Fig. 8.** Steady-state shear at T = 180 °C: (a) Viscosity *versus* shear rate (b) First normal stress difference ($N_1$) *versus* shear rate.

was predominant. In the latter case, greater free volume is associated with branching compared to recombination between macroradicals, which leads to higher viscosities.

To confirm the above-mentioned analyses, rheological analyses were performed in the oscillatory state, as shown in Fig. 9.

Fig. 9a displays the G′ curves for the studied samples, enabling a comparative analysis for the different curve behaviors. According to the literature, linear polymers exhibit a G′ proportional to approximately $\omega^2$ at low rates on a log–log plot (Han, 2007). As shown in Fig. 9b, the terminal slope at low rates for neat PLA was 1.3, while for the PLA_0.5_3 sample, it was 1.4. These results indicate minimal branching in the structure of the latter sample, suggesting that its chain structure is closer to that of neat PLA. Conversely, the other modified samples demonstrated slopes between 0.4 and 0.5. Terminal slopes between 1.03 and 1.39 have been reported in the literature for PLA and have been directly associated with the branched nature of the materials (Nouri et al., 2015), indicating that these samples possess more complex structures.

As shown in Fig. 9b, PLA_0_0 presented a typical viscous fluid behavior in low frequencies in the terminal zone. For the modified samples, tanδ is lower but still presents a viscous fluid behavior for sample PLA_0.5_3. For samples PLA_0.5_1 and PLA_1.5_3, values of tanδ are low in low frequencies, decreasing to values near 1, forming a Plateau. These results indicate a likely formation of long chain branches for these formulations, with higher relaxation times.

Ultimately, the van Gurp-Palmen (vGP) plot and Cole-cole are commonly used to distinguish between linear and branched polymer structures (Tiwary et al., 2021). In vGP, the behavior of linear polymers is characterized by a phase angle δ close to 90° at low |G*| values, which is typical of linear polyethylenes. The extent of deviation from this behavior is indicative of the presence of branched structures (Wang et al., 2011). Fig. 9c presents the vGP plot for the samples analyzed. The graph illustrates that neat PLA exhibits behavior consistent with linear polymers, displaying a well-defined terminal zone near the 90° phase angle. However, the modified samples demonstrate a noticeable deviation from this pattern, particularly evident in the PLA_1.5_3 and PLA_0.5_1 samples, suggesting the presence of branches. At equivalent values of the complex modulus, these samples exhibit a reduced phase angle, indicating a less viscous behavior compared to neat PLA. Similar deviations from the behavior of neat PLA have been observed by other researchers (P. Li et al., 2021a, 2021b, 2020a).

Cole-Cole analysis (Fig. 9d) suggests the same interpretations, as it is possible to observe the formation of arcs for PLA_0_0, a typical behavior of linear polymers (P. Li et al., 2020b). Sample PLA_0.5_3 also presents an arc form with a bigger radius, indicating a higher molar mass. For formulations PLA_0.5_1 and PLA_1.5_3, it is not possible to observe the complete formation of arcs due to their very high relaxation times, suggesting the formation of long chain branches, making the material more elastic. Tian et al. also observed the same evidence for long-chain branch formation (Tian et al., 2006). The authors evaluated the chain extension of PP during the reactive process with 2,5-dimethyl-2,5(*tert*-butylperoxy) hexane peroxide and pentaerythritol triacrylate (PETA).

This analysis allows the correlation of the observed rheological properties with the different concentrations of GMA and DCP. Given that all modified samples exhibited higher viscosity and elasticity than neat PLA, comparisons will be focused only on the modified samples. Three distinct relationships can be identified between the concentrations of GMA and DCP to elucidate their respective influences:

- **Influence 1 –** Increasing in peroxide (PLA_**0.5**_3 vs. PLA_**1.5**_3)**:** There is a significant increase in both complex viscosity and storage modulus. The substantial deviation observed in the vGP graph indicates the presence of branching structures.
- **Influence 2 –** Increasing in GMA (PLA_0.5_**1** vs. PLA_0.5_**3**): A notable decrease in complex viscosity and storage modulus is

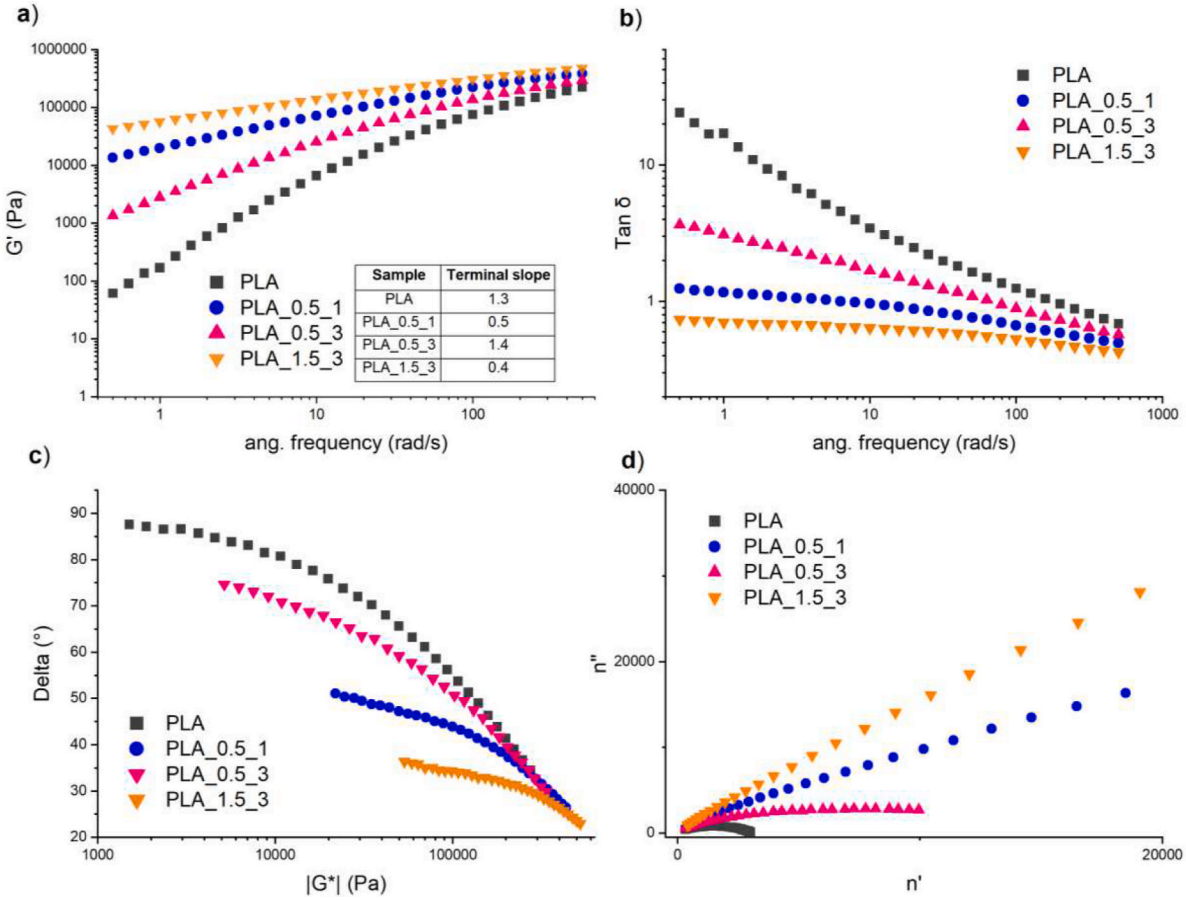


**Fig. 9.** Rheological analysis in the oscillatory state for modified and neat PLA samples at T = 180 °C: a) G' *versus* angular frequency; b) tanδ *versus* angular frequency; c) van Gurp-Palmen plot; d) Cole-Cole.

observed, with the behavior approaching that of linear polymers, as depicted in the vGP and Cole-Cole graph.

- **Influence 3 –** Increasing in peroxide and GMA (PLA_**0.5**_**1** vs. PLA_**1.5**_**3**): There is an increase in complex viscosity, with a predominance of storage modulus over loss modulus, suggesting higher elasticity. The behavior in the vGP and Cole-Cole graph is similar for both samples, yet both exhibit significant deviations from the behavior of linear polymers. This suggests the presence of long chain branches and recombination between macroradicals without the formation of crosslinking.

Understanding the influence of GMA and DCP on the structure of PLA and, consequently, the rheological properties of the material, provides valuable insights into how these factors will impact the cellular structures of the resulting foams.

### 3.3. *Influence of chemical modification on PLA foams*

Finally, to evaluate whether chemical modification varying concentration of GMA and peroxide onto PLA would support extensional deformation caused by decompression of supercritical $CO_2$, samples were foamed, as described in Methodology, and SEM analysis with low magnification is presented in Fig. 10. Only formulation PLA_1.5_1 could not be foamed because it was crosslinked.

In general, the literature presents that chemical modification of PLA with various chain extenders and/or peroxides results in foams with more controlled structures due to the increase in melt strength (P. Li et al., 2021b; Venkatesan et al., 2021). As can be seen in Fig. 10 (at low magnification), unmodified PLA has large cells with heterogeneous shapes and misshapen regions where thick cell walls can be seen (identified by the red circles). The modified samples, on the other hand, show smaller cell sizes, in which sample PLA_0.5_3 has a more heterogeneous morphology when compared to the other two, with ruptured structures, that lead to large voids, as identified by the red arrows. Less obviously, sample PLA_1.5_3 also shows heterogeneity in its cell structures, with larger ruptured cells. In general, sample PLA_0.5_1 shows smaller cell sizes with greater homogeneity.

These observations were confirmed by the characterization of the structures. Fig. 11 and Fig. 12 illustrate, respectively, higher magnification images (1200x) as well as their respective cell size distributions and the foam density, cell density values, volume expansion ratio and average cell size.

As can be seen, the modified PLA was able to produce microcellular foams, with average sizes of around 15 and 20 μm. According to the statistical test, all the samples showed a significant difference in size, including neat PLA.

According to the cell size distribution graphs, it is clear that neat PLA resulted in cells with larger sizes and a wide distribution, which is a result of the heterogeneity of the structures. With the addition of the modifiers, the cells presented a decrease in size, in which sample PLA_0.5_1 resulted in the smallest average and narrowest distribution.

The statistical test showed that the significant difference between the densities of the samples is mainly between the modified ones. Following the same idea as before, it is possible to correlate the structures achieved to the concentrations of peroxide and GMA.

- **Influence 1** – Increase in peroxide (PLA_**0.5**_3 vs. PLA_**1.5**_3): increase in VER, decrease in cell size and increase in cell density.

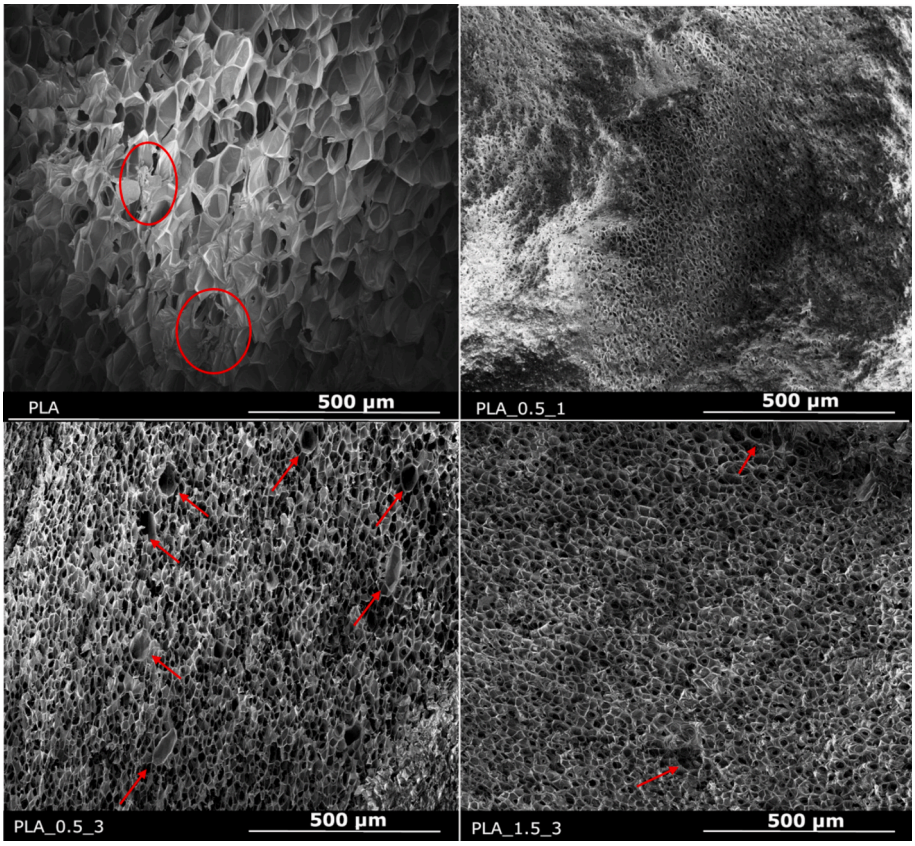


**Fig. 10.** SEM images of neat and modified PLA at a magnification of 250x.

- **Influence 2** – Increase in GMA (PLA_0.5_**1** vs. PLA_0.5_**3**): decrease in VER, increase in cell size and decrease in cell density.
- **Influence 3** – Increase in peroxide and GMA (PLA_**0.5_1** vs. PLA_**1.5_3**): Increase in VER, increase in cell size and decrease in cell density.

It is therefore understood that in Influence 1, the expressive increase in viscosity and elasticity resulted in an increase in VER and a decrease in cell size, which increased cell density. Therefore, cell density was decisive in the material's foamability. Influence 2, on the other hand, caused a decrease in VER, which must be the result of the decrease in viscosity and elasticity of the material, which did not have enough resistance to prevent the cells from coalescing. As a result, the decrease in cell density resulted in a decrease in VER. Finally, Influence 3, as well as Influence 1, also increased VER, but with an increase in cell size, which must be the result of the increased elasticity of the samples and the lower degree of heterogeneous nucleation of cells, due to their lower crystallinity (Pang et al., 2022).

In this context, it is known in the literature that, for semi-crystalline polymers, crystallization can occur during the gas saturation phase, which will have a direct influence on the structures formed. It is therefore essential to investigate the presence of crystals during the foaming of the material.

In order to understand the role of crystals during the foaming process, a DSC analysis of the foams was carried out. All the foamed samples, including neat PLA, showed an increase in the percentage of crystallinity after the foaming process (PLA: 31 %; PLA_0.5_1: 30 %; PLA_0.5_3: 33 %; PLA_1.5_3: 25 %). The PLA_1.5_3 sample showed the smallest increase in crystallinity, which can be explained by the complex branched structure due to grafting and possible recombination of macroradicals, which, even with the lubricating effect of sc-$CO_2$, was unable to organize itself at the same level as the other samples. However, it is possible to state that, even if in different magnitudes, all the samples had a heterogeneous cell nucleation process. This may explain, for example, why neat PLA was able to expand, even though it had low elasticity in the melt. According to Li and coauthors (B. Li et al., 2019), increasing the number of crystals can increase the elastic nature of the material, reducing cell rupture. For the other modified samples, other factors influence foaming due to changes in the structure of the material, which was not the case for neat PLA.

Another observation is that even though the PLA_1.5_3 sample had the highest storage modulus and viscosity values, the resulting structures did not have the smallest cell sizes or the narrowest distribution. This can be explained by the smaller number of crystals present during saturation with sc-$CO_2$. The lower the concentration of crystals, the lower the nucleation, so the cells can grow more, which explains the lower cell density for this sample compared to PLA_0.5_1.

In general, with the observations made, the difference in crystallinity between the PLA_0.5_1 and PLA_1.5_3 samples seems to have been the decisive factor in determining the cell structures formed since the experiments were all carried out under the same conditions. The two samples showed the greatest elasticity and viscosity, but the higher percentage of crystallinity in the PLA_0.5_1 sample may have been the reason why the cells showed smaller sizes and a more homogeneous distribution.

For PLA_0.5_3, crystallinity was the highest among the samples, which helped with cell nucleation and increased melt strength. However, the strength was not enough to prevent the cells from coalescing.

These results show that the foaming of polymeric materials is complex and depends on several factors. The same factors will not always have the same magnitude of contribution (Pang et al., 2022). For the present study, a relationship could be established between the complex viscosity of the material and the percentage of crystallinity achieved during saturation with sc-$CO_2$, as seen in Fig. 13.

As can be seen, crystallinity close to 30 % with a complex viscosity of around $10^6$ Pa resulted in homogeneous structures with small cells and

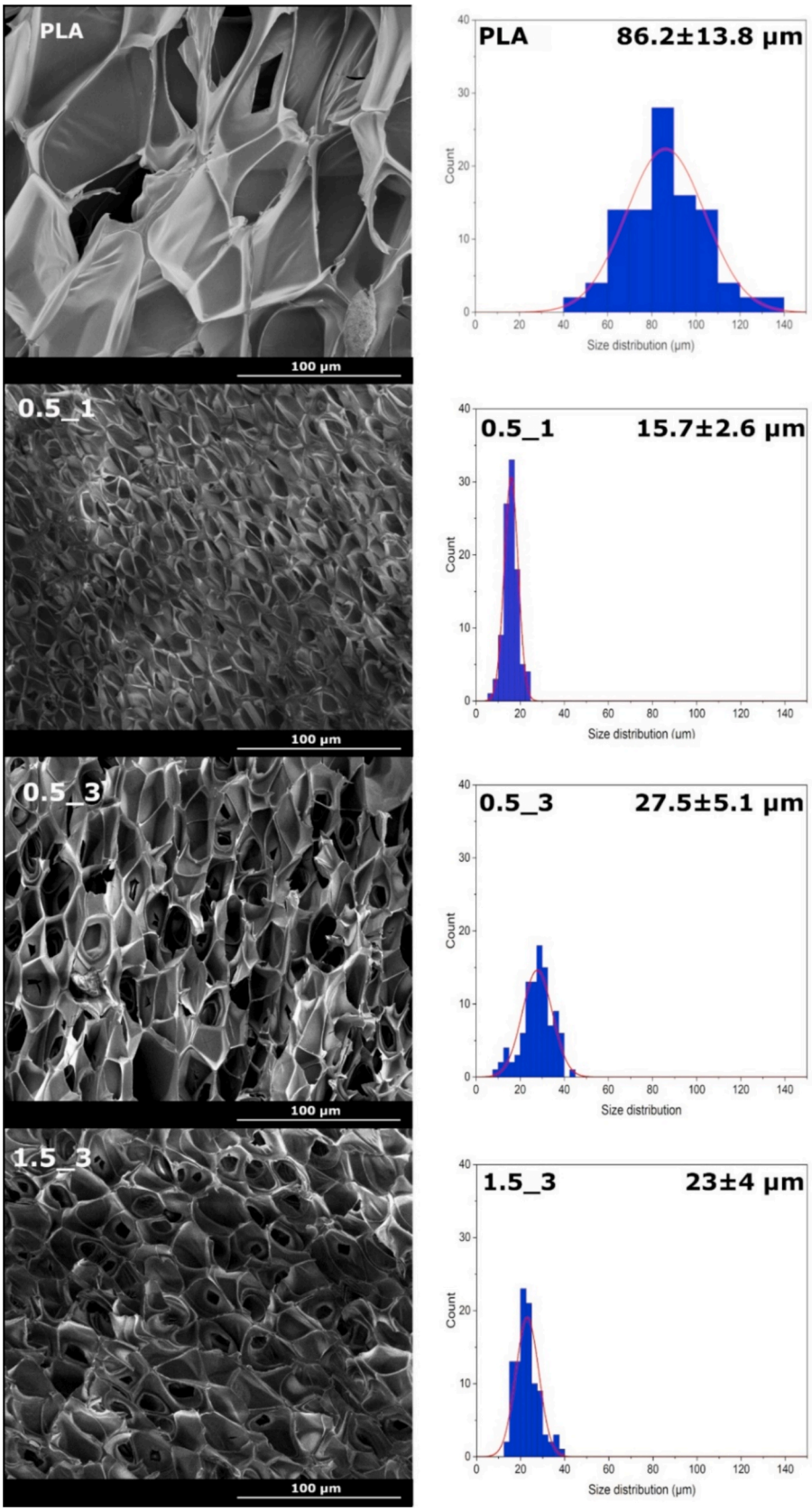


**Fig. 11.** Morphologies of cell structures obtained by SEM at 1200x magnification, with graphs of the respective cell size distributions.

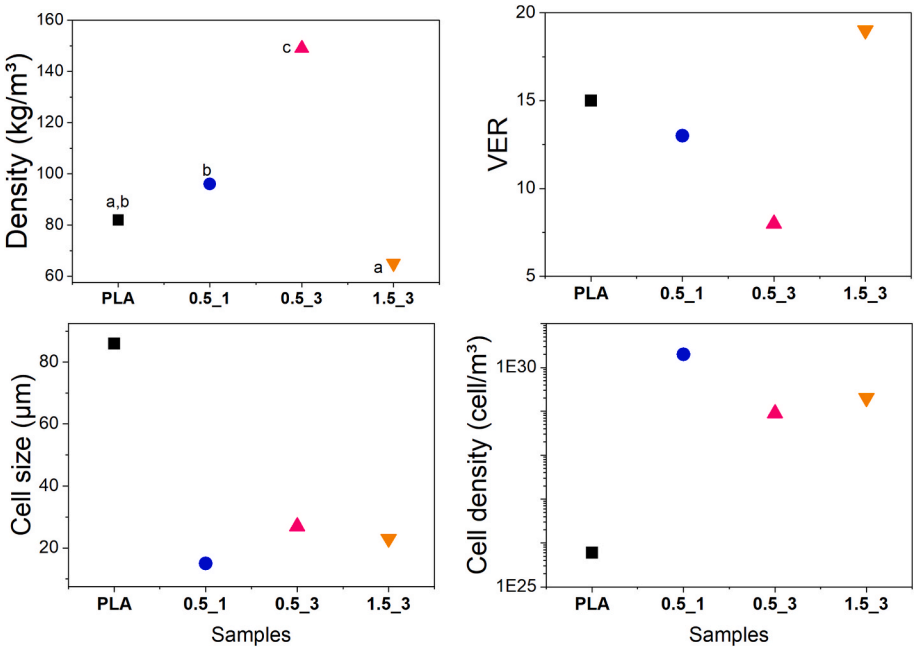


**Fig. 12.** Density, volume expansion ratio (VER), cell size and cell density values. Equal letters correspond to statistically similar samples.

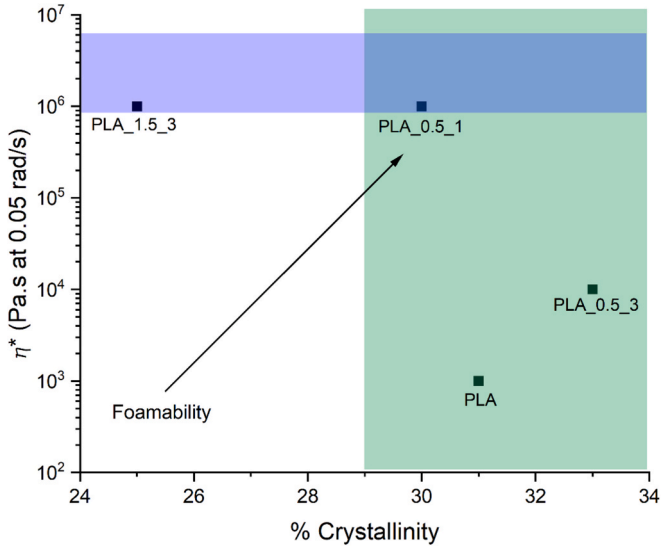


**Fig. 13.** Relationship between crystallinity and complex viscosity for the production of foams with controlled and uniform sizes.

closed pores. Chen and colleagues (Chen et al., 2021) analyzed PLA with different levels of D-isomer to understand the role of crystallinity in foams. The authors also observed that a minimum crystallinity limit resulted in closed and homogeneous pore structures, whereas for the low crystallinity grade, it was between 18 and 24 %. The values for the more crystalline grade were between 32 and 39 %.

This relationship shows that the increase in complex viscosity and crystallinity led to the production of suitable structures. However, it is known that this ratio can only increase up to an optimum condition, as very high viscosities can make the melt strength too high for the material to expand (Y. Li et al., 2020), and very high crystallinity can make it difficult for $CO_2$ to dissolve in the material (Li et al., 2017), reducing foamability.

## 4. Conclusions

This paper presented the results obtained from the chemical modification of PLA by reactive processing, using GMA as the modifying monomer and DCP as the initiator, and the influence of these modifications on the PLA chemical structures and foamability.

Concerning the chemical modification, the study showed that there is competition between reactions during reactive processing, and depending on the concentrations of the reagents, this competition will favor the recombination of macroradicals, and/or the formation of branches, and/or linear reactions.

The presence of DCP isolated at the concentrations studied (0.5 and 1.5 phr) resulted in the sample's crosslinking; the higher its concentration, the higher the crosslinking content. This result is due to the large number of macroradicals formed, which recombine to create a complex network. However, for most of the samples, the crosslinking decreased to close to zero when GMA was added at different concentrations.

It is, therefore, clear that there is an optimum relationship between the concentrations of reagents in which the amount of macroradicals formed and the amount of GMA available in the medium will dictate the types of chemical structures that will be formed. Consequently, these relationships will result in different thermal and rheological properties.

For the production of polymeric foams, in which the presence of long branches is essential for the material to have high extensional viscosity, samples 0.5_1 and 1.5_3 resulted in more homogeneous cell structures when compared to the other samples. This must be due to the presence of long branches and the recombination of macroradicals, resulting in high apparent viscosity and elasticity. For the neat PLA and 0.5_3 samples, which presented the lowest viscosities and rheological behavior typical of linear polymers, the resulting foams had heterogeneous cells with thick walls.

The properties resulting from modification with GMA and DCP cannot be directly related to the final cellular structures formed, as the crystallization of the material during the $CO_2$ saturation stage will also influence the process. It can be concluded that crystallinity can favor the formation of small, homogeneous structures at a given viscosity since high crystallinity at low viscosities results in large structures with many coalesced cells. On the other hand, high viscosities hinder the formation of crystals, reducing bubbles' nucleation and resulting in larger cells.

Other factors can influence the process, such as temperature, time, pressure, among others, however, in this investigation, these factors were not varied.

Therefore, this study showed that there is an optimum conditions window that combines viscosity *versus* crystallinity to achieve morphologies with uniform structures. Understanding the relationship between polymer properties and the cell structures formed is essential for determining the properties of the final foam products, which can be applied in various sectors. In addition, the fact that the material comes from renewable sources and can biodegrade under composting conditions also helps to mitigate the problems currently faced by the excessive use of conventional plastic products. Finally, this investigation brings novelties to the understanding of different chemical structures formed as different ratios between GMA and DCP are adopted and their influence on the final cellular structures of modified PLA foams.

## CRediT authorship contribution statement

**Ana Beatriz Valim Suquisaqui:** Writing – original draft, Methodology, Investigation, Formal analysis, Data curation, Conceptualization. **Lívia Maria Garcia Gonçalves:** Methodology, Investigation. **Laís Taguchi Possari:** Methodology, Investigation. **Eliada Andrade Silva:** Investigation, Data curation. **Benedito dos Santos Lima Neto:** Investigation, Data curation. **Rosario Elida Suman Bretas:** Writing – review & editing, Supervision, Investigation. **Paulo de Tarso Vieira e Rosa:** Writing – review & editing, Supervision, Investigation. **Sílvia Helena Prado Bettini:** Writing – review & editing, Supervision, Resources, Project administration, Funding acquisition, Conceptualization.

## Declaration of competing interest

The authors declare the following financial interests/personal relationships which may be considered as potential competing interests: Silvia Helena Prado Bettini reports financial support and equipment, drugs, or supplies were provided by State of Sao Paulo Research Foundation. Silvia Helena Prado Bettini reports financial support and equipment, drugs, or supplies were provided by National Council for Scientific and Technological Development. If there are other authors, they declare that they have no known competing financial interests or personal relationships that could have appeared to influence the work reported in this paper.

## Acknowledgment

This study was financed in part by the Coordenação de Aperfeiçoamento de Pessoal de Nível Superior - Brasil (CAPES) - Finance Code 001; by the São Paulo Research Foundation (FAPESP) – grant no. 2020/07633–2; and by the Brazilian National Council for Scientific and Technological Development (CNPq) through the INCT Circularity in Polymer Materials – grant no. 406925/2022–4. We thank the Laboratory of Structural Characterization, Department of Materials Engineering, Federal University of São Carlos, for the use of its general facilities.

## Data availability

Data will be made available on request.

## References

Ansari, A.I., Sheikh, N.A., 2023. A Review on Different Approaches for Foam Fabrication. J. Inst. Eng. Ser. C 104, 1219–1245. https://doi.org/10.1007/s40032-023-00998-x.

Auras, R., Lim, L.-T., Selke, S.E.M., Tsuji, H., 2010. Poly(lactic acid): synthesis, structures, properties, processing and application. John Wiley & Sons.

Banerjee, R., Ray, S.S., 2020. Foamability and Special Applications of Microcellular Thermoplastic Polymers: A Review on Recent Advances and Future Direction. Macromol. Mater. Eng. 305, 1–49. https://doi.org/10.1002/mame.202000366.

Bianchin, O.S., Melo, G.H.F., Bretas, R.E.S., 2021. Effect of MWCNT carboxyl functionalization on the shear rheological and electrical properties of HMS-PP/MWCNT foams. J. Cell. Plast. 57, 210–235. https://doi.org/10.1177/0021955X20943096.

Champeau, M., Thomassin, J.M., Tassaing, T., Jérôme, C., 2015. Drug loading of polymer implants by supercritical CO2 assisted impregnation: A review. J. Control. Release 209, 248–259. https://doi.org/10.1016/j.jconrel.2015.05.002.

Chen, J., Yang, L., Mai, Q., Li, M., Wu, L., Kong, P., 2021. Foaming behavior of poly (lactic acid) with different D-isomer content based on supercritical CO2-induced crystallization. J. Cell. Plast. 57, 675–694. https://doi.org/10.1177/0021955X20950242.

Corre, Y.M., Maazouz, A., Duchet, J., Reignier, J., 2011. Batch foaming of chain extended PLA with supercritical CO2: Influence of the rheological properties and the process parameters on the cellular structure. J. Supercrit. Fluids 58, 177–188. https://doi.org/10.1016/j.supflu.2011.03.006.

Cui, W., Wei, X., Luo, J., Xu, B., Zhou, H., Wang, X., 2022. CO2-assisted fabrication of PLA foams with exceptional compressive property and heat resistance via introducing well-dispersed stereocomplex crystallites. J. CO2 Util. 64. https://doi.org/10.1016/j.jcou.2022.102184.

Dirlam, P.T., Goldfeld, D.J., Dykes, D.C., Hillmyer, M.A., 2019. Polylactide Foams with Tunable Mechanical Properties and Wettability using a Star Polymer Architecture and a Mixture of Surfactants. ACS Sustain. Chem. Eng. 7, 1698–1706. https://doi.org/10.1021/acssuschemeng.8b05461.

Dong, M., Wang, G., Zhang, X., Tan, D., Kumar, J.P., D., Ren, J., Colorado, H., Hou, H., Toktarbay, Z., Guo, Z.,, 2023. An overview of polymer foaming assisted by supercritical fluid. Adv. Compos. Hybrid Mater. 6, 1–22. https://doi.org/10.1007/s42114-023-00790-6.

Forghani, E., Azizi, H., Karabi, M., Ghasemi, I., 2016. Compatibility, morphology and mechanical properties of polylactic acid/polyolefin elastomer foams. J. Cell. Plast. 54, 235–255. https://doi.org/10.1177/0021955X16681450.

Gonçalves, L.F.F.F., Reis, R.L., Fernandes, E.M., 2024. Forefront Research of Foaming Strategies on Biodegradable Polymers and Their Composites by Thermal or Melt-Based Processing Technologies: Advances and Perspectives. Polymers (basel). 16. https://doi.org/10.3390/polym16091286.

Hamielec, A.E., Gloor, P.E., Zhu, S., 1991. Kinetics of, free radical modification of polyolefins in extruders – chain scission, crosslinking and grafting. Can. J. Chem. Eng. 69, 611–618. https://doi.org/10.1002/cjce.5450690302.

Han, C.D., 2007. Rheology and Processing of Polymeric Materials. Oxford University Press Inc.

Hopmann, C., Schippers, S., Höfs, C., 2015. Influence of recycling of poly(lactic acid) on packaging relevant properties. J. Appl. Polym. Sci. 132, np-n/a. https://doi.org/10.1002/app.41532.

Jin, F.L., Zhao, M., Park, M., Park, S.J., 2019. Recent trends of foaming in polymer processing: A review. Polymers (basel). 11. https://doi.org/10.3390/polym11060953.

Kangwanwatthanasiri, P., Suppakarn, N., Ruksakulpiwat, C., Ruksakulpiwat, Y., 2015. Glycidyl methacrylate grafted polylactic acid: Morphological properties and crystallization behavior. Macromol. Symp. 354, 237–243. https://doi.org/10.1002/masy.201400094.

Kuska, R., Milovanovic, S., Frerich, S., Ivanovic, J., 2019. Thermal analysis of polylactic acid under high CO2 pressure applied in supercritical impregnation and foaming process design. J. Supercrit. Fluids 144, 71–80. https://doi.org/10.1016/j.supflu.2018.10.008.

Lee, S.-T., 2017. Polymeric foams: Innovations in Processes. CRC Press, Boca Raton, Technologies and Products.

Li, J., Liao, X., Yang, Q., Li, G., 2017. Crystals in situ induced by supercritical co2 as bubble nucleation sites on spherulitic plla foam structure controlling. Ind. Eng. Chem. Res. 56, 11111–11124. https://doi.org/10.1021/acs.iecr.7b02348.

Li, J., Song, Y., Cai, Y., 2020a. Focus topics on microplastics in soil: Analytical methods, occurrence, transport, and ecological risks. Environ. Pollut. 257, 113570. https://doi.org/10.1016/j.envpol.2019.113570.

Li, M., Li, S., Liu, B., Jiang, T., Zhang, D., Cao, L., He, L., Gong, W., 2021a. Rheological behavior, crystallization properties, and foaming performance of chain-extended poly (lactic acid) by functionalized epoxy. RSC Adv. 11, 32799–32809. https://doi.org/10.1039/d1ra06382k.

Li, P., Zhang, W., Kong, M., Lv, Y., Huang, Y., Yang, Q., Li, G., 2021b. Ultrahigh performance polylactide achieved by the design of molecular structure. Mater. Des. 206. https://doi.org/10.1016/j.matdes.2021.109779.

Li, P., Zhang, W., Zhu, X., Kong, M., Lv, Y., Huang, Y., Gong, P., Li, G., 2020b. Simultaneous Improvement of the Foaming Property and Heat Resistance in Polylactide via One-step Branching Reaction Initiated by Cyclic Organic Peroxide. Ind. Eng. Chem. Res. 59, 2934–2945. https://doi.org/10.1021/acs.iecr.9b05784.

Nouri, S., Dubois, C., Lafleur, P.G., 2015. Effect of chemical and physical branching on rheological behavior of polylactide. J. Rheol. N. Y. N. Y). 59, 1045–1063. https://doi.org/10.1122/1.4922486.

Pang, Y., Cao, Y., Zheng, W., Park, C.B., 2022. A comprehensive review of cell structure variation and general rules for polymer microcellular foams. Chem. Eng. J. 430. https://doi.org/10.1016/j.cej.2021.132662.

Rigolin, T.R., Costa, L.C., Bettini, S.H.P., 2021. Chemically modified poly(lactic acid): structural approach employing two distinct monomers. J. Polym. Res. 28, 1–10. https://doi.org/10.1007/s10965-021-02504-2.

Rigolin, T.R., Costa, L.C., Venâncio, T., Perlatti, B., Bettini, S.H.P., 2019. The effect of different peroxides on physical and chemical properties of poly(lactic acid) modified with maleic anhydride. Polymer (guildf). 179. https://doi.org/10.1016/j.polymer.2019.121669.

Rojas, A., Torres, A., Galotto, M.J., Guarda, A., Julio, R., 2020. Supercritical impregnation for food applications: a review of the effect of the operational variables

on the active compound loading. Crit. Rev. Food Sci. Nutr. 60, 1290–1301–2022. https://doi.org/10.1080/10408398.2019.1567459.
Lee S.-T. Park C.B. Ramesh N.S. Polymeric foams: science and technology 2007 CRC Press - Taylor & Francis Group Boca Raton.
Södergård, A., Stolt, M., 2002. Properties of lactic acid based polymers and their correlation with composition. Prog. Polym. Sci. 27, 1123–1163. https://doi.org/10.1016/S0079-6700(02)00012-6.
Souza F.M. Desai Y. Gupta R.K. Polymeric foams: fundamentals and types of foams 2023 American Chemical Society Washington, DC 10.1021/bk-2023-1439.ch001.
Standau, T., Zhao, C., Castellón, S.M., Bonten, C., Altstädt, V., 2019b. Chemical modification and foam processing of polylactide (PLA). Polymers (basel). 11. https://doi.org/10.3390/polym11020306.
Thanh, C.N., Chaiwat, R., Yupaporn, R., 2016. Effect of glycidyl methacrylate (GMA) content on grafting yield and mechanical properties of GMA Grafted Poly(Lactic Acid) Prepared by Melt Mixing Method. Key Eng. Mater. 709, 27–31. https://doi.org/10.4028/www.scientific.net/KEM.709.27.
Tian, J., Yu, W., Zhou, C., 2006. The preparation and rheology characterization of long chain branching polypropylene. Polymer (guildf). 47, 7962–7969. https://doi.org/10.1016/j.polymer.2006.09.042.
Tiwary, P., Najafi, N., Kontopoulou, M., 2021. Advances in peroxide-initiated graft modification of thermoplastic biopolyesters by reactive extrusion. Can. J. Chem. Eng. 99, 1870–1884. https://doi.org/10.1002/cjce:24080.
Venkatesan, K.B., Karkhanis, S.S., Matuana, L.M., 2021. Microcellular foaming of poly (lactic acid) branched with food-grade chain extenders. J. Appl. Polym. Sci. 138. https://doi.org/10.1002/app.50686.
Wang, G., Zhao, J., Wang, G., Mark, L.H., Park, C.B., Zhao, G., 2017. Low-density and structure-tunable microcellular PMMA foams with improved thermal-insulation and compressive mechanical properties. Eur. Polym. J. 95, 382–393. https://doi.org/10.1016/j.eurpolymj.2017.08.025.
Wang, L., He, Y., Jiang, T., Zhang, X., Zhang, C., Peng, X., 2019a. Morphologies and properties of epoxy/multi-walled carbon nanotube nanocomposite foams prepared through the free-foaming and limited-foaming process. Compos. Sci. Technol. 182, 107776. https://doi.org/10.1016/j.compscitech.2019.107776.
Wang, X., Li, Y., Jiao, Y., Zhou, H., Wang, X., 2019b. Microcellular Foaming Behaviors of Poly (Lactic Acid)/Low-Density Polyethylene Blends Induced by Compatibilization Effect. J. Polym. Environ. 27, 1721–1734. https://doi.org/10.1007/s10924-019-01466-3.
Wang, X., Mi, J., Wang, J., Zhou, H., Wang, X., 2018. Multiple actions of poly(ethylene octene) grafted with glycidyl methacrylate on the performance of poly(lactic acid). RSC Adv. 8, 34418–34427. https://doi.org/10.1039/C8RA07510G.
Wang, Y., Yang, L., Niu, Y., Wang, Z., Zhang, J., Yu, F., Zhang, H., 2011. Rheological and Topological Characterizations of Electron Beam Irradiation Prepared Long-Chain Branched Polylactic Acid. J. Appl. Polym. Sci. 122, 1857–1865. https://doi.org/10.1002/app.
Xu, T., Tang, Z., Zhu, J., 2012. Synthesis of polylactide-graft-glycidyl methacrylate graft copolymer and its application as a coupling agent in polylactide/bamboo flour biocomposites. J. Appl. Polym. Sci. 125, E622–E627. https://doi.org/10.1002/app.36808.
Yan, Z., Liao, X., He, G., Li, S., Guo, F., Zou, F., Li, G., 2020. Green and High-Expansion PLLA/PDLA Foams with Excellent Thermal Insulation and Enhanced Compressive Properties. Ind. Eng. Chem. Res. 59, 19244–19251. https://doi.org/10.1021/acs.iecr.0c02492.
Yang, Y., Li, X., Zhang, Q., Xia, C., Chen, C., Chen, X., Yu, P., 2019. Foaming of poly (lactic acid) with supercritical CO2: The combined effect of crystallinity and crystalline morphology on cellular structure. J. Supercrit. Fluids 145, 122–132. https://doi.org/10.1016/j.supflu.2018.12.006.
Zhou, M., Zhou, P., Xiong, P., Qian, X., Zheng, H., 2015. Crystallization, rheology and foam morphology of branched PLA prepared by novel type of chain extender. Macromol. Res. 23, 231–236. https://doi.org/10.1007/s13233-015-3018-0.